Molecular characterization of type I IFN-induced cytotoxicity in bladder cancer cells reveals biomarkers of resistance

Jennifer L. Green,[1,3] Robin E. Osterhout,[1,3] Amy L. Klova,[1] Carsten Merkwirth,[1] Scott R.P. McDonnell,[1] Reza Beheshti Zavareh,[1] Bryan C. Fuchs,[1] Adeela Kamal,[1] and Jørn S. Jakobsen[2]

[1]Ferring Research Institute, San Diego, CA, USA; [2]Ferring Pharmaceuticals, International PharmaScience Center, Copenhagen, Denmark

Although anti-tumor activities of type I interferons (IFNs) have been recognized for decades, the molecular mechanisms contributing to clinical response remain poorly understood. The complex functions of these pleiotropic cytokines include stimulation of innate and adaptive immune responses against tumors as well as direct inhibition of tumor cells. In high-grade, Bacillus Calmette-Guérin (BCG)-unresponsive non-muscle-invasive bladder cancer, nadofaragene firadenovec, a non-replicating adenovirus administered locally to express the *IFNα2b* transgene, embodies a novel approach to deploy the therapeutic activity of type I IFNs while minimizing systemic toxicities. Deciphering which functions of type I IFN are required for clinical activity will bolster efforts to maximize the efficacy of nadofaragene firadenovec and other type I IFN-based therapies, and inform strategies to address resistance. As such, we characterized the phenotypic and molecular response of human bladder cancer cell lines to IFNα delivered in multiple contexts, including adenoviral delivery. We found that constitutive activation of the type I IFN signaling pathway is a biomarker for resistance to both transcriptional response and direct cytotoxic effects of IFNα. We present several genes that discriminate between sensitive and resistant tumor cells, suggesting they should be explored for utility as biomarkers in future clinical trials of type I IFN-based anti-tumor therapies.

INTRODUCTION

Non-muscle-invasive bladder cancer (NMIBC) represents approximately 75% of all new cases of bladder cancer.[1] The standard of care treatment for high-grade NMIBC is endoscopic tumor resection followed by intravesical treatment with the attenuated bacterium Bacillus Calmette-Guérin (BCG). While this treatment regimen is effective for many patients, approximately one-third of patients become resistant over time.[2]

Nadofaragene firadenovec (rAd-IFNα/Syn3) is a non-replicating and non-integrating type 5 adenovirus packaged with the *IFNα2b* transgene that is delivered locally to provide sustained production of IFNα2b in the bladder urothelium.[3,4] This novel therapy for patients with BCG-unresponsive NMIBC recently demonstrated efficacy in a Phase 3 clinical

trial.[5] Although the efficacy, safety, and administration frequency of nadofaragene firadenovec compares favorably with other contemporary bladder-sparing therapies, some patients do not respond for unknown reasons.[5] Furthermore, urine IFNα2b concentrations did not correlate with clinical response in a Phase 2 trial,[6] suggesting that tumor-intrinsic or immunological mechanisms of resistance may exist.

Type I IFNs, including IFNα and IFNβ, are pleiotropic cytokines that induce transcription of a large group of interferon-stimulated genes (ISGs). Although type I IFNs are approved for treating a variety of malignancies,[7] understanding the mechanisms leading to clinical efficacy is hampered by the diverse functions of these cytokines. Type I IFNs directly inhibit tumor cells by inducing cytotoxicity and growth arrest. They also activate natural killer (NK) cells, enhance cross-priming of CD8^{+} T cells by dendritic cells, and sustain proliferation and activation of T cells.[8,9] While much is known about how tumor-intrinsic properties can determine the outcome of tumor rejection by T cells and NK cells (e.g., expression of the immune checkpoint ligand programmed death-ligand 1 [PD-L1],[10] or major histocompatibility complex class I [MHC-I][11]), little is known about the mechanisms that provide cancer cells with resistance to the direct effects of type I IFN.

In the context of bladder cancer, the IFNα protein induces cell death in some bladder cancer cell lines, but not others,[12–14] whereas adenoviral delivery of the *IFNα2b* transgene (Ad-IFNα2b) and conditioned media produced by cells transduced with Ad-IFNα2b are reported to have unique cytotoxic properties distinct from the IFNα2b protein, and are able to overcome resistance to IFNα2b.[12,15–17] The clinical activity of nadofaragene firadenovec could conceivably be attributed to any of the above mechanisms (i.e., analogous to exposure to IFN protein, adenovirus, or conditioned media), as it likely transduces both tumor cells and surrounding normal urothelial cells that condition the tumor

Table 1. Panel of human bladder cancer cell lines

Cell line	Year	Gender	Stage	Grade	Location	Molecular Subtype[a]	Reference
RT4	1970	Male	pT1	G1-2	bladder	LumP	[18]
UM-UC-6	1982	Male	Nr	nr	bladder	Ba/Sq	[19]
SW-780	1974	Female	Nr	G1	bladder	LumP	[20]
UM-UC-4	1982	Female	NA	NA	lymph node	LumU	[19]
UM-UC-10	1982	Nr	Nr	G3	bladder	Ba/Sq	[21]
UM-UC-3	1982	Male	pT2-T4	nr	bladder	Ba/Sq	[19]
TCC-SUP	1974	Female	Nr	G4	bladder	Ba/Sq	[22]
T24	1970	Female	pTa	G3	bladder	Ba/Sq	[23]
SCaBER	1976	Male	Nr	nr	bladder	Ba/Sq	[24]
HT-1197	1972	Male	pT2	G4	bladder	Ba/Sq	[25]
HT-1376	1973	Female	≥pT2	G3	bladder	Ba/Sq	[25]
J82	1972	Male	pT3	G3	bladder	Ba/Sq	[26]

nr, not reported/unknown; NA = not applicable.

[a]The Consensus MIBC classifier (Kamoun et al.[27]) was applied to RNA-seq data from untreated cell lines, which were classified as Luminal papillary (LumP), Luminal unstable (LumU), or Basal/squamous (Ba/Sq).

microenvironment (TME). The goal of the present study was to better understand the spectrum of cellular responses to these various types of IFNα exposure and to identify candidate biomarkers that can correlate sensitivity with a therapeutic response. A better understanding of the anti-tumor effects of IFNα2b and Ad-IFNα2b in the context of bladder cancer will assist in the design and analysis of future clinical trials and enable optimization of this novel treatment approach.

RESULTS

IFNα does not inhibit G1-S transition in bladder cancer cells

Anti-proliferative effects of type I IFN have been reported for diverse cell types, including bladder cancer; however, some of the earlier reports described assays that do not distinguish between cell proliferation arrest and cell death.[13,14,17] To clarify the effects of type I IFN on proliferation of bladder cancer cells, we chose an assay (5-ethynyl-2′-deoxyuridine [EdU] incorporation) that measures cell-cycle progression rather than cell number, because cell number can be a compound effect of cell proliferation and/or viability. We assembled a panel of 12 diverse human bladder cancer cell lines (Table 1) and the non-transformed immortalized cell line SV-HUC-1, and measured cell-cycle progression from G1 to S phase in response to stimuli. The CDK4/6 inhibitor palbociclib was used as a positive control for cell-cycle arrest.[28] While several cell lines were sensitive to cell-cycle inhibition by 1 μM palbociclib (>50%), no cell line was inhibited by recombinant human IFNα2b (rhIFNα2b) (Figure 1), suggesting that the previously described, direct inhibition of bladder tumor growth may be more attributable to the cytotoxic effects of type I IFN, rather than to the anti-proliferative effects.

Cytotoxic response to IFNα and Ad-IFNα is variable among bladder cancer cell lines

As rhIFNα2b, Ad-IFNα2b, and conditioned media produced by Ad-IFNα2b transduced cells are reported to have distinct anti-tumor effects,

we characterized the ability of these various treatments to induce cytotoxicity in our human bladder cancer cell line panel. Cells were exposed to rhIFNα2b, tumor necrosis factor-related apoptosis-inducing ligand (TRAIL), Ad-IFNα2b, Ad-GFP, and conditioned media produced by Ad-IFNα2b- or Ad-GFP-transduced SV-HUC-1 cells for 48 h (Figures 2A–2G). Cytotoxicity was quantified by CytoTox-Glo Assay (Promega) with treatment doses and multiplicity of infection (MOI) selected to achieve maximal effects based on previous publications.[12,17] The concentration of rhIFNα2b used here (100,000 U/mL) was similar to the concentration of IFNα2b protein measured in the urine of patients treated with nadofaragene firadenovec.[6] A variable response to rhIFNα2b was observed with the greatest effect in the RT4 cell line and no effect in the J82 cell line. Response to rhIFNα2b was highly correlated with response to Ad-IFNα2b (Pearson r = 0.87), although the magnitude of the cytotoxic effect was greater with Ad-IFNα2b (Figure 2H). Similarly, response to rhIFNα2b was highly correlated with response to conditioned media produced by Ad-IFNα2b-transduced cells (Pearson r = 0.97), suggesting that the cytotoxic activity in Ad-IFNα2b conditioned media is derived primarily from secreted IFNα2b protein, rather than from an unidentified bystander factor as previously proposed.[17] There was no cytotoxicity induced by conditioned media produced by Ad-GFP-transduced cells. While smaller in magnitude, the response to Ad-GFP was highly correlated with response to Ad-IFNα2b (Pearson r = 0.90), suggesting that Ad-IFNα2b cytotoxicity partially reflects cytotoxicity from adenoviral infection, independent of IFNα2b. To characterize the relative contribution of the vector alone, we compared cytotoxicity in RT4 induced by Ad-IFNα2b, Ad-GFP, and Ad-empty (Figure 2I). There was much lower cytotoxicity induced by Ad-empty, than by Ad-IFNα2b or Ad-GFP, suggesting that the cytotoxicity from the adenovirus may be due in part to exogenous transgene overexpression, for example by diversion of cellular resources away from production of endogenous genes and proteins or by induction of endoplasmic reticulum stress.
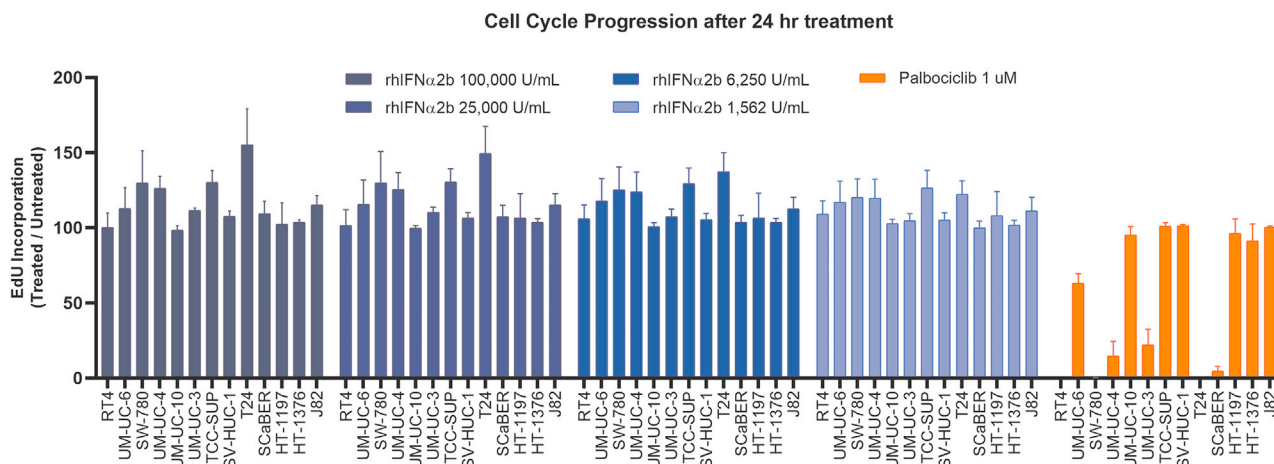
Figure 1. IFNα does not alter proliferation in bladder cancer cell lines

Proliferation was measured by EdU (a nucleoside analog of thymidine) incorporation following 24 h of exposure to palbociclib or rhIFNα2b. EdU incorporation was calculated by dividing the number of EdU-positive nuclei by the total number of nuclei. The graph depicts EdU incorporation in treated cells divided by EdU incorporation in untreated cells multiplied by 100 for each cell line. Results are presented as mean ± SD from three independent experiments performed in quadruplicate. EdU, 5-ethynyl-2′-deoxyuridine; h, hour; IFN, interferon; SD, standard deviation.

The cytotoxic effects of type I IFNs are often mediated by TRAIL.[12] In agreement with a partial dependency on TRAIL induction, we observed a weak but statistically significant correlation between response to TRAIL and response to rhIFNα2b (Pearson r = 0.66). As reported previously, the UM-UC-10 cell line exemplifies a cell line that is sensitive to rhIFNα2b, but not to exogenous TRAIL (Figures 2B and 2C).[12] Of note, the TRAIL receptor DR4 (TNFRSF10A) was not differentially expressed between IFNα-sensitive and -resistant cell lines when measured by immunoblot (see Figure 5B).

Transcriptional response to IFNα differs between sensitive and resistant cell lines

To further investigate the molecular mechanisms of tumor-intrinsic sensitivity or resistance to IFNα-induced cytotoxicity, we compared the transcriptional response to rhIFNα2b between the most sensitive and most resistant cell lines, RT4 and J82, respectively. Cells were treated with 1,000 U/mL or 10,000 U/mL rhIFNα2b, then RNA was collected at 4 h, 8 h, and 24 h post-treatment and subjected to RNA-sequencing (RNA-seq) analysis. rhIFNα2b induced a robust dose- and time-dependent transcriptional response in RT4 cells, with predominant increases in mRNA concentration of known ISGs (Figure 3A). Surprisingly, many of the known ISGs induced in RT4 were already expressed at high levels in untreated J82 cells and showed minimal induction with rhIFNα2b treatment. Expression changes for several classic ISGs (*IFI27, STAT1, BST2*) were verified by quantitative polymerase chain reaction (qPCR) and were consistent with the RNA-seq results (Figure 3B).

Constitutive IFNα pathway activation correlates with tumor-intrinsic resistance

The differential ISG expression between RT4 and J82 led to the hypothesis that constitutive type I IFN pathway activation might be a common mechanism of rhIFNα2b resistance in bladder cancer. We therefore examined the transcriptional response to rhIFNα2b in the full panel of bladder cancer cell lines (Figure 4A). Following treatment with 10,000 U/mL rhIFNα2b for 24 h, there was a substantial increase in ISG expression in some of the cell lines, while others showed only minor changes in gene expression. As seen with J82, several other cell lines also displayed high ISG expression in the absence of rhIFNα2b treatment, suggesting that the type I IFN pathway is constitutively active in these cells. To characterize basal type I IFN pathway activity in the cell line panel, we defined an IFNα response signature composed of the top 65 genes upregulated upon rhIFNα2b treatment that also had high basal expression in a subset of the cell lines. Using this IFNα response signature score, we categorized the cell lines into two groups, "ISG-low" and "ISG-high." Gene set enrichment analysis (GSEA) was performed to assess pathway-level differences between the two groups, in the absence of treatment (Figure 4B). The top pathway enriched in the "ISG-high" cell lines was the Hallmark IFNα response pathway. Suppressed pathways in ISG-high cell lines include MYC targets and oxidative phosphorylation. Notably, although cytotoxic response to rhIFNα2b appeared as a continuum in the cell line panel (Figure 2B), categorization based on IFNα response signature score segregated the cell lines into two groups with significantly different cytotoxic responses (Figure 4C), with the ISG-high cell lines showing resistance to IFNα-induced cytotoxicity.

IFNα response signature predicts IFNα resistance in additional tumor types

To assess the generality of constitutive type I IFN pathway activity as a candidate biomarker of resistance, we used the IFNα response signature to investigate the correlation between type I IFN pathway activity and IFNα resistance in other tumor types. GSE21158 is an independent microarray dataset comprising cell lines determined to be
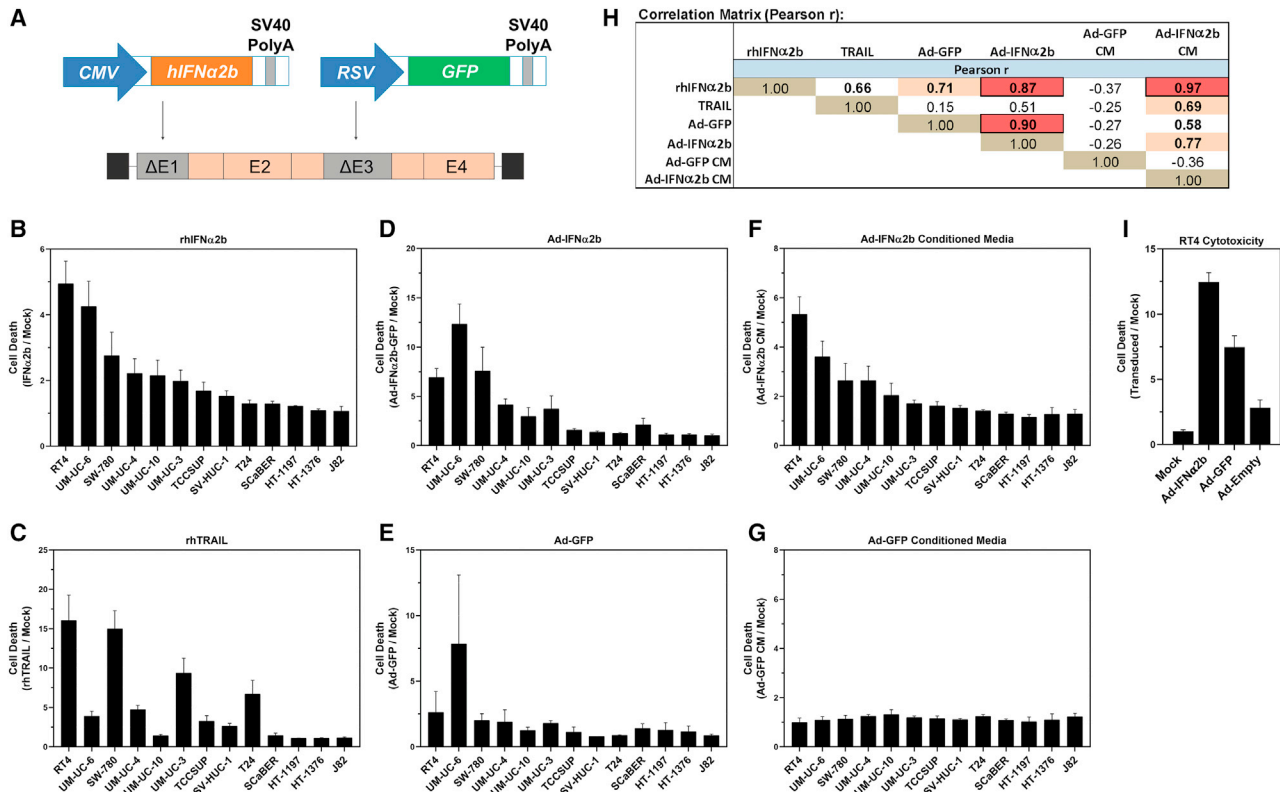
Figure 2. IFNα is cytotoxic to a subset of bladder cancer cell lines in multiple contexts

(A) Schematic of adenoviral tool vectors. The Ad-IFNα2b vector includes hIFNα2b driven by a CMV promoter inserted into the E1 region and GFP driven by the RSV promoter inserted into the E3 region. The Ad-GFP vector includes an empty E1 region and GFP driven by the RSV promoter inserted into the E3 region. Both tool viruses lack viral E1 and E3. (B–G) Cells were exposed to (B) 100,000 U/mL rhIFNα2b, (C) 50 ng/mL TRAIL, (D) Ad-IFNα2b (MOI = 100), (E) Ad-GFP (MOI = 100) and conditioned media (CM) produced by (F) Ad-IFNα2b or (G) Ad-GFP transduced SV-HUC-1 cells. Cytotoxicity is reported as the relative fraction of dead cells after 48 h of treatment. Results are presented as mean ± SD from independent experiments performed in triplicate; N = 2 or 3 for Ad-GFP, N = 3 for all other treatments. (H) Pairwise correlation analysis was performed for all treatments and the Pearson correlation coefficient was determined. Bold indicates $P < 0.05$. (I) Cells were exposed to Ad-IFNα2b, Ad-GFP, or Ad-empty (MOI = 100 for all); cytotoxicity is reported as the relative fraction of dead cells after 48 h of treatment.

Ad, adenovirus vector; CMV, cytomegalovirus; GFP, green fluorescent protein; rhIFNα2b, recombinant human interferon alpha 2b, rhTRAIL, recombinant human TNF-related apoptosis-inducing ligand; RSV, respiratory syncytial virus; SV40 Poly(A), simian virus 40 polyadenylated tail.

sensitive or resistant to IFNα using orthogonal assays.[29] Cell lines in this study are derived from melanoma, lung, colorectal, and pancreatic tumors. For each untreated cell line, the IFNα signature was applied to calculate an IFNα response score. Note that 32 of 65 genes in the signature were missing from the GSE21158 array. Nonetheless, the reduced signature scores were able to discriminate sensitive and resistant cell lines (Figure 4D).

IFNα response signature in The Cancer Genome Atlas samples

To characterize the IFNα response signature in patient bladder cancer tumors, we scored The Cancer Genome Atlas (TCGA) primary tumors against the cell-line-derived signature. Variability in IFNα pathway activation could be reflective of differences in tumor purity, immune and/or stromal cell infiltration, or tumor-intrinsic characteristics. Tumor purity of each primary tumor was assessed using the Consensus Purity Estimation algorithm;[30] stromal and immune infil-

tration were quantified using the ESTIMATE method.[31] This analysis showed that higher immune infiltration and lower tumor purity were positively associated with elevated IFNα response scores (Figure 4E). Surprisingly, tumors with low immune and stromal infiltration scores showed a broad range of IFNα response scores (Figure 4F), suggesting that in some primary tumors, cancer cells may exhibit high tumor-intrinsic IFN pathway activity in the absence of infiltrating cells. This result is consistent with findings by Liu et al. characterizing a 38-gene ISG core signature across primary TCGA tumor lineages, patient-derived tumor xenograft, and cancer cell lines models,[32] supporting the hypothesis that a subset of bladder cancer tumors express ISGs constitutively in the absence of an immune component.

Implications for resistance to anti-tumor immune response

In the context of an immune-competent TME, the anti-tumor effects of IFNα extend beyond direct cytotoxicity. For example, it is well
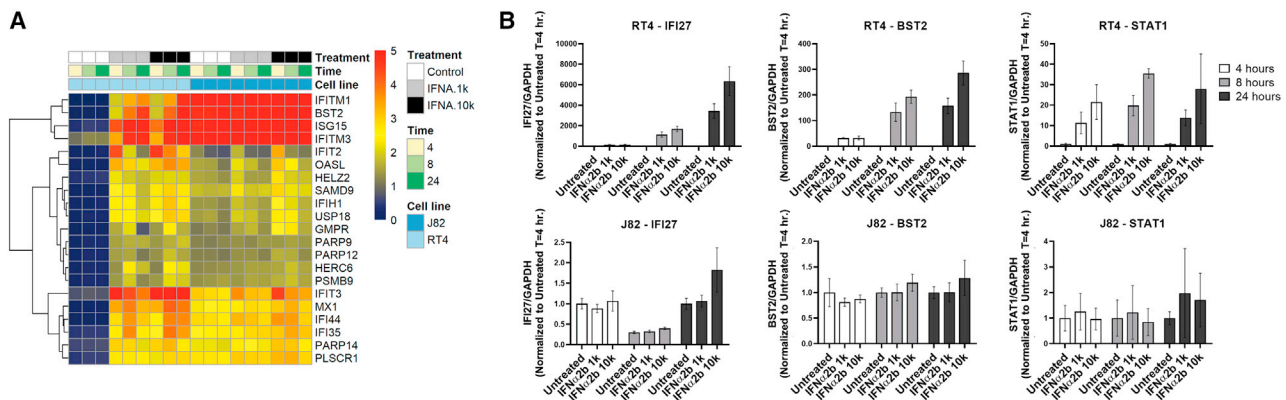
Figure 3. Differential expression of ISGs in bladder cancer cell lines

(A) RNA-seq was performed on RT4 and J82 cells following treatment with rhIFNα2b at 1,000 U/mL (1 k) or 10,000 U/mL (10 k) for 4, 8, or 24 h. Heatmap shows top differentially expressed genes in the canonical IFNα response pathway. ISGs are expressed at low levels in a sensitive cell line (RT4) and increase over time following treatment with INFα. Non-responsive cell lines (e.g., J82) express ISGs constitutively (ISG-high). (B) Changes in gene expression levels of *IFI27, STAT1,* and *BST2* measured by RT-qPCR relative to GAPDH (housekeeping gene) following treatment with IFNa2b. Triplicate wells were seeded for three conditions for each time point: Untreated, 1000 U/mL rhIFNα2b, and 10,000 U/mL rhIFNα2b. Each of the three conditions were harvested at every time point. The y axis indicates the ratio of the expression of the gene-of-interest in relation to the housekeeping gene GAPDH, normalized to the untreated sample at time = 4 h. Results are presented as the mean ± SD from three independent RNA samples analyzed in triplicate (N = 3). GAPDH, glyceraldehyde 3-phosphate dehydrogenase; IFNα, interferon alpha; ISG, interferon-stimulated gene; rhIFNα2b, recombinant human interferon alpha 2b; RNAseq, ribonucleic acid sequencing; RT-qPCR, real-time-quantitative polymerase chain reaction; SD, standard deviation

known that type I IFNs induce MHC-I expression, which promotes recognition of tumor cells by CD8^{+} T cells.[9] In addition, type I IFNs are reported to induce expression of the immune checkpoint receptor ligand PD-L1, which inhibits CD8^{+} T cell-mediated killing.[33,34] To gain a broader view of how constitutive ISG expression might contribute to tumor-cell recognition by the adaptive immune system, we examined the expression of the MHC-I genes *HLA-A, HLA-B, HLA-C* and the common *B2M* subunit as well as the gene encoding PD-L1 (*CD274*) in the bladder cancer cell line panel (Figure 5A). *HLA-B, HLA-C,* and *B2M* were significantly upregulated by rhIFNα2b in the ISG-low cell lines. Although the MHC-I genes were not significantly upregulated by rhIFNα2b in the ISG-high cell lines, the basal levels of expression in these cell lines were comparable to the levels in stimulated ISG-low cells. There was not a statistically significant difference in *CD274* expression with rhIFNα2b treatment in either group.

Potential molecular mechanisms of constitutive IFNα pathway activation

It was recently reported that mismatch repair-deficient (MMRd) tumors have increased cytosolic DNA that leads to activation of the cyclic GMP-AMP synthase-stimulator of interferon genes (cGAS-STING) pathway and subsequently to elevated type I IFN expression.[35] Increased expression of type I IFN genes due to cGAS-STING activity could potentially manifest as the ISG-high state we observed here. Of the 13 type I IFN genes, *IFNB1, IFNE,* and *IFNK* were expressed at extremely low levels in both ISG-low and ISG-high cell lines (Table 2), while the remaining type I IFN genes were undetectable in any cell line. The exception was *IFNK,* which was moderately expressed in the SCaBER cell line (not shown). Although we cannot exclude relevant differences in type I IFN ligand expression between ISG-high and ISG-low

cell lines that are below the detection threshold, we did not find evidence supporting a mechanism whereby cGAS-STING drives the ISG-high phenotype by inducing type I IFN expression. In agreement with an earlier report that bladder cancer cell sensitivity to the direct effects of IFNα is not determined by receptor number or ligand affinity,[36] the genes encoding the type I IFN receptor, *IFNAR1* and *IFNAR2,* were not elevated in the ISG-high cell lines compared with the ISG-low cell lines (Table 2). IFNAR1 protein expression was confirmed by immunoblot (see Figure 5B).

We next considered whether loss of a negative regulator might contribute to the ISG-high state. As the observed lack of type I IFN ligand or receptor overexpression suggests that constitutive pathway activation occurs downstream of ligand binding, we examined expression of negative regulators of the type I IFN response (*SOCS1, SOCS3, IRF2, PIAS, SMAD2, SMAD3, PKD2, PTPN1, PTPN2, PTPN6, PTPN11, USP18*),[37] but did not find reduced expression in the ISG-high cell lines (Table 2). Interestingly, the negative regulator *USP18,* also an ISG, was expressed at higher levels in the ISG-high cell lines than the ISG-low cell lines. The response of bladder cancer cell lines and tumors to chemotherapy, inhibitors of epidermal growth factor receptor or type-3 fibroblast growth factor receptor (FGFR3) was previously shown to be associated with molecular subtype and epithelial versus mesenchymal differentiation.[38,39] To evaluate whether molecular subtype is associated with the ISG-high phenotype and response to IFNα, a muscle invasive bladder cancer (MIBC) consensus classifier was applied to RNA-seq data from untreated cell lines, which were classified as Basal/Squamous (Ba/Sq), Luminal papillary (LumP) or Luminal unstable (LumU) (Table 1).[27] While all of the resistant cell lines were of the Ba/Sq subtype, and all of the luminal cell lines (LumP and LumU) were sensitive, there is
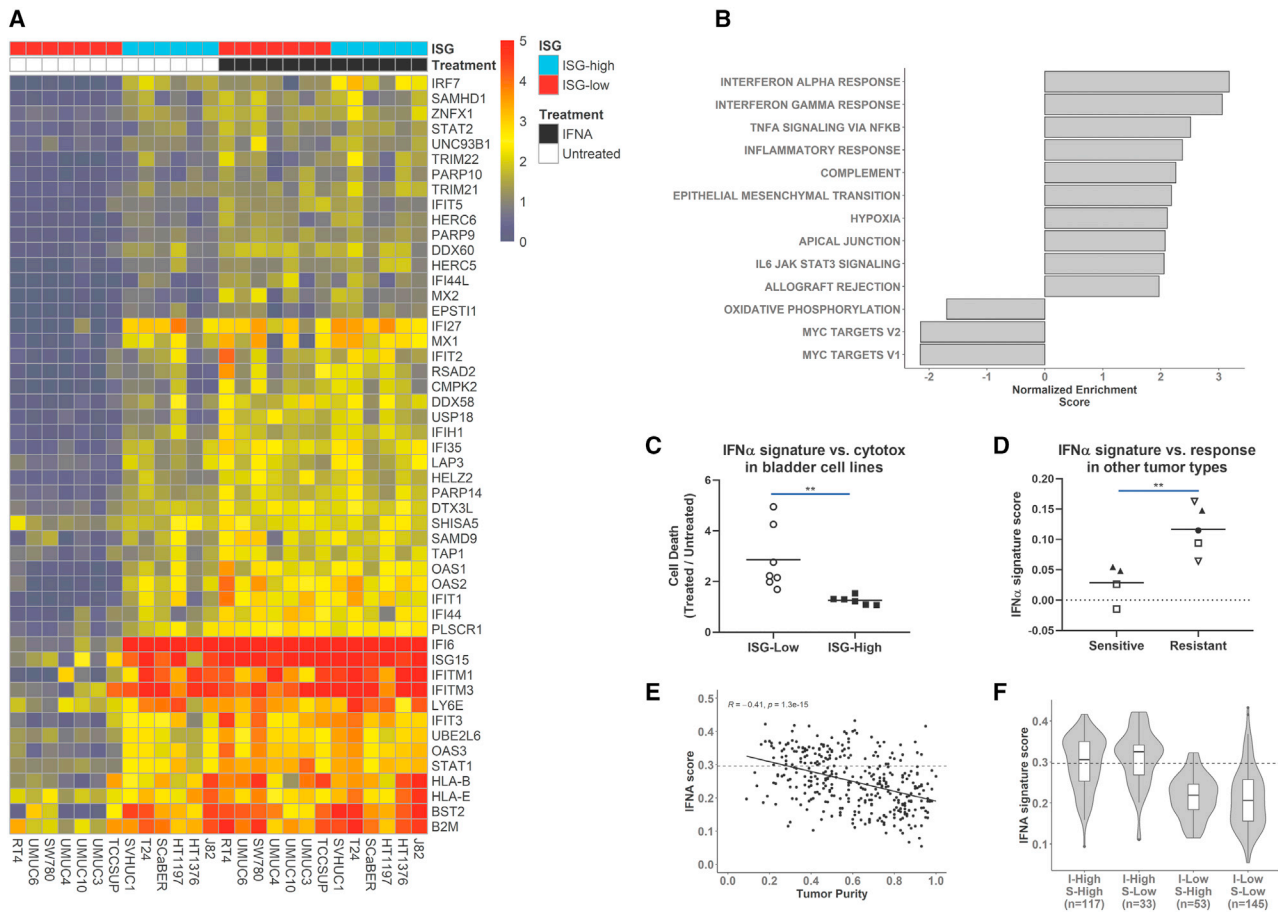
Figure 4. Constitutive ISG expression is associated with resistance to INFα treatment

(A) RNA-seq was performed on all cell lines following treatment with 40,000 U/mL rhIFNα2b for 24 h (except for RT4, which received 10,000 U/mL rhIFNα2b for 24 h). Heatmap shows the top 50 genes that discriminate between the "ISG-high" and "ISG-low" cell lines in untreated and IFNα-treated conditions. ISG-high cell lines and treatment condition are indicated in color bars across the top of the figure; ISG-high or ISG-low cell line samples are colored blue or red, respectively; untreated or IFNA-treated samples are colored white or black, respectively. (B) GSEA pathway analysis of "ISG-high" versus "ISG-low" cell lines; normalized enrichment scores of top 10 (if applicable) MSigDB "Hallmark" enriched pathways are shown. (C) IFNα-induced cytotoxicity was significantly diminished in bladder cell lines with an ISG-high expression pattern. Data points show the mean rhIFNα2b-induced cytotoxicity of each cell line from Figure 2B. (D) The 65-gene IFNα signature scores were calculated for each cell line in the GSE21158 microarray analysis. Cell line tissue of origin is indicated by point shape (filled circle ● = colorectal, open triangle ▽ = lung, filled triangle ▼ = pancreatic, open square □ = melanoma). Data points represent the mean score for each cell line, categorized as IFNα sensitive or resistant by the referenced dataset. (E) IFNα signature score in TCGA primary bladder cancer tumors (n = 348) is anticorrelated with tumor purity (Pearson's correlation coefficient $R = -0.41$). Dotted line represents the score cutoff for ISG-high tumors as defined in the materials and methods section. Each dot represents a tumor sample. (F) Association between IFNα signature score and immune and stromal infiltration in TCGA primary bladder cancer tumors. Immune and stromal scores are classified into subgroups as described in the materials and methods section. I-high is immune-high, I-low is immune-low, S-high is stromal-high and S-low is stromal low. Overlaid boxplots show median and interquartile range for each immune/stromal subgroup. GSEA, gene set enrichment analysis; ISG, interfon signature gene; rhIFNα2b, recombinant human interferon alpha 2b; TCGA, The Cancer Genome Atlas.

insufficient subtype representation in our panel to draw definitive conclusions about the contribution of molecular subtype to IFNα response. Peroxisome proliferation-activated receptor-gamma (PPAR-γ), a nuclear receptor strongly associated with luminal subtypes,[27,40] was not differentially expressed between ISG-high and ISG-low cell lines as measured by gene expression (Table 2) nor by immunoblot (Figure 5B). Likewise, E-cadherin and vimentin, markers of epithelial and mesenchymal differentiation, respectively, were also not differentially expressed between ISG-high and ISG-

low cell lines as measured by gene expression (Table 2) nor by immunoblot (Figure 5B).

ISG expression can be sustained by prolonged expression of signal transducer and activator of transcription 1 (STAT1), as part of a positive feedback mechanism.[41] STAT1 gene expression and protein levels were higher in the untreated ISG-high cell lines than in the untreated ISG-low cell lines (Figures 4A and 5B). To determine whether the abundant STAT1 protein in ISG-high cell lines reflects STAT1
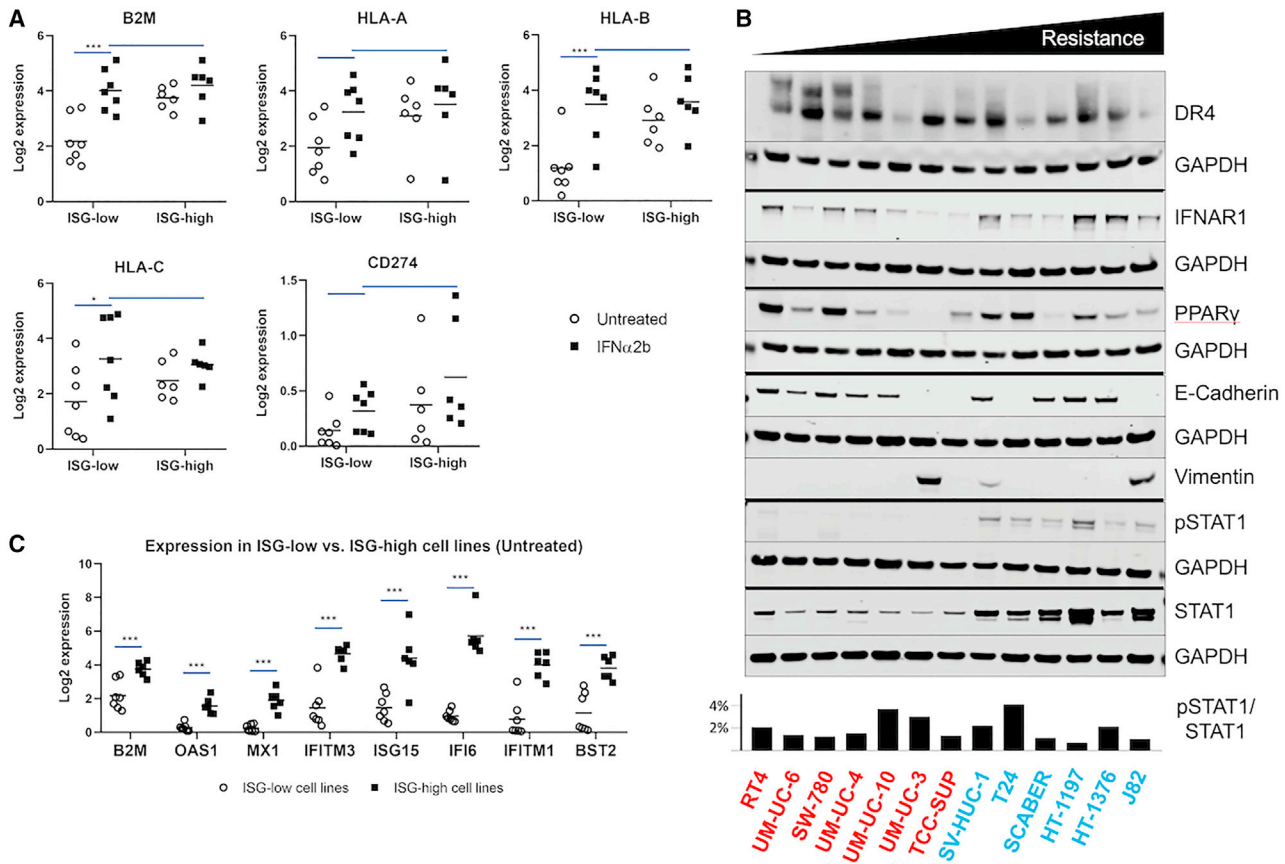
Figure 5. Expression analysis of immunoregulatory genes, candidate biomarkers and mechanism-associated proteins

(A) Expression of MHC Class I genes and immune checkpoint ligand PD-L1 (*CD274*) in untreated and rhIFNα2b-treated cell lines, grouped by ISG-high or -low. (B) Immunoblots of cellular lysates obtained from unstimulated cell lines. Labels of ISG-high cell lines are blue; labels of ISH-low cell lines are red. The bar graph shows the pTyr701-STAT1 signal (normalized to GAPDH) as a percentage of the total STAT1 signal (also normalized to GAPDH). (C) Expression of candidate biomarkers in untreated ISG-low versus ISG-high cell lines. (A and C) Each data point reflects the mean Log2 expression value in a cell line measured by RNA-seq (n = 3). Black horizontal lines represent the mean score for each cell line category, *$P < 0.05$, ***$P < 0.001$, see the materials and methods for determination of significance.

DR4, death receptor 4 (TRAIL receptor 1); GAPDH, glyceraldehyde 3-phosphate dehydrogenase; IFNAR1, interferon alpha receptor 1; ISG-high, high basal expression of interferon-stimulated genes; ISG-low, low basal expression of interferon-stimulated genes; MHC-I, major histocompatibility complex class I; PD-L1, programmed cell death-ligand; PPARγ, peroxisome proliferator- activated receptor gamma; rhIFNα2b, recombinant human interferon alpha 2b; pTyr701, phosphorylation of tyrosine at position 701; STAT1, signal transducer and activator of transcription 1.

protein that has been activated by type I IFN signaling, we measured STAT1 phosphorylation at tyrosine residue Tyr701, which is rapidly increased following exposure to type I IFN.[42] Although Tyr701-phosphorylated STAT1 (pTyr701-STAT) was more abundant in the ISG-high than the ISG-low cell lines (Figure 5B), the relative amount of pTyr701-STAT to total STAT1 was not higher in the ISG-high cell lines. It has been reported that unphosphorylated STAT1 (U-STAT1), in complex with interferon regulatory factor 9 (IRF9), can stimulate constitutive IFN-independent ISG expression to protect against viral infection.[43] The increased levels of total STAT1 in ISG-high cell lines, without enrichment of pTyr701-STAT, in conjunction with the lack of elevated type I IFN or IFNAR1 expression noted above, are consistent with a U-STAT1-mediated mechanism of ISG upregulation.

Characterization of individual ISGs as candidate biomarkers of IFNα resistance

Determining the clinical relevance of resistance to the tumor-intrinsic effects of type I IFNs requires measurement of candidate biomarkers in samples from treated patients with known clinical outcomes. In cases in which tissue sample is limited, or RNA might be of poor quality, it can be preferable to use a targeted approach aimed at measuring a small number of genes or proteins, rather than detecting a gene expression signature. Therefore, we examined the degree to which individual genes from the IFNα response signature correlate with cytotoxic response. We selected five ISGs with high basal expression (*IFI6, IFITM3, ISG15, IFITM1, BST2*) in the ISG-high bladder cell lines as well as classic ISGs (*B2M, OAS1, MX1*)[44–47] that were previously used in clinical trials of type I IFN proteins, and compared their

Table 2. Mean expression levels of select genes in untreated ISG-high and ISG-low cell lines

Gene Symbol	ISG-low (log2 TPM)	ISG-high (log2 TPM)	Fold-Change (ISG-High/ISG-Low)[a]	Gene Symbol	ISG-Low (log2 TPM)	ISG-High (log2 TPM)	Fold-Change (ISG-High/ISG-Low)[a]
B2M	2.27	3.74	**2.77**[b]	PIAS1	0.23	0.24	1.01
BST2	1.2	3.79	**6.02**[b]	PKD2	0.3	0.44	1.1
CD274	0.18	0.41	1.17	PPARG	0.78	0.73	0.97
CDH1	1.41	1.56	1.11	PTPN1	1.08	1.43	1.27
HLA-A	2.02	3.08	2.08	PTPN11	1.48	1.3	0.88
HLA-B	1.24	2.89	**3.14**[b]	PTPN2	0.28	0.26	0.99
HLA-C	1.76	2.44	1.6	PTPN6	0.28	0.23	0.97
IFI6	1	5.7	**25.99**[b]	SMAD2	0.17	0.15	0.99
IFITM1	0.8	3.99	**9.13**[b]	SMAD3	0.8	0.92	1.09
IFITM3	1.51	4.63	**8.69**[b]	SOCS1	0.08	0.2	1.09
IFNAR1	0.6	0.54	0.96	SOCS3	0.4	0.36	0.97
IFNAR2	0.02	0.01	0.99	STAT1	1.12	2.55	**2.69**[b]
IFNB1	0	0.01	1.01	TNFRSF10A	0.62	0.41	0.86
IFNE	0.03	0.02	0.99	TNFRSF10B	1.33	0.9	0.74
IFNK	0	0.32	1.25	TNFSF10	0.23	1.18	**1.93**[b]
IRF2	0.51	0.58	1.05	TP53	0.84	0.82	0.99
ISG15	1.52	4.38	**7.26**[b]	USP18	0.26	0.94	**1.6**[b]
MX1	0.26	1.88	**3.07**[b]	VIM	0.5	0.34	0.9
OAS1	0.28	1.55	**2.41**[b]	PIAS1	0.23	0.24	1.01

ISG, interferon-stimulated gene; TPM, transcript count per million.
[a]Fold-change in mean expression of selected genes in untreated ISG-high versus untreated ISG-low cell lines.
[b]Indicates the gene meets the criteria for differential expression (false discovery adjusted p value <0.05).

expression levels with the ISG-low cell lines (Figure 5C). Of these genes, OAS1, MX1, IFI6, and BST2 perfectly segregated the two groups, with IFI6 showing the best separation between the groups and the highest expression levels in resistant cells.

DISCUSSION

The anti-tumor activity of IFN-based therapies is complex and likely involves both immune-mediated and immune-independent mechanisms. To characterize tumor-intrinsic resistance to the direct effects of type I IFNs, we evaluated the phenotypic and molecular response of a panel of human bladder cancer cell lines to IFNα delivered in various formats. The pattern of cytotoxic response among the cell lines to the rhIFNα2b protein, Ad-IFNα2b and Ad-IFNα2b conditioned media was qualitatively similar, suggesting that the IFNα2b transgene product is primarily responsible for the cytotoxic response seen from the adenovirus agents. Interestingly, we found that cell lines most resistant to IFNα treatment display constitutive ISG expression.

We explored several mechanisms that might cause or be associated with constitutive type I IFN signaling in some bladder cancer cell lines. Type I IFN ligands and receptors were not overexpressed in ISG-high cell lines. STAT1 mRNA and protein levels were elevated in ISG-high cell lines, but pTyr701-STAT1 was not enriched. Together, these results are consistent with a mechanism whereby

U-STAT-1 promotes ISG expression in the absence of type I IFN, as has been reported to protect against viral infection.[43]

Type I IFN-induced cytotoxicity has several potential contributions to the clinical activity of IFN-based anti-tumor therapies, the first of which is direct ablation of tumor cells. Second, dying cells release tumor antigens and immunostimulatory factors, which can facilitate an anti-tumor immune response. In addition to resistance to the cytotoxic effects of type I IFN, ISG-high cells showed minimal transcriptional response to rhIFNα2b, which may also have implications for anti-tumor immunity. Induction of MHC-I expression by type I IFNs increases antigen display and recognition of tumor cells by CD8$^+$ T cells.[9] Thus, diminished MHC-I induction by IFNα in cells with constitutive pathway activity could theoretically hamper part of the type I IFN anti-tumor activity mediated by the adaptive immune system. However, because the levels of MHC-I gene expression in untreated ISG-high cell lines are similar to those in rhIFNα2b-treated ISG-low cells, the action of type I IFNs on dendritic cells in the TME could be sufficient to induce tumor rejection by the adaptive immune system, even against tumors resistant to the direct effects of type I IFN (Figure 6). Therefore, MHC-I mediated recognition of tumor cells, while potentially enhanced in ISG-low tumors, is not expected to be impaired in ISG-high tumors. In addition to MHC-I, type I IFN is also reported to induce expression of the checkpoint
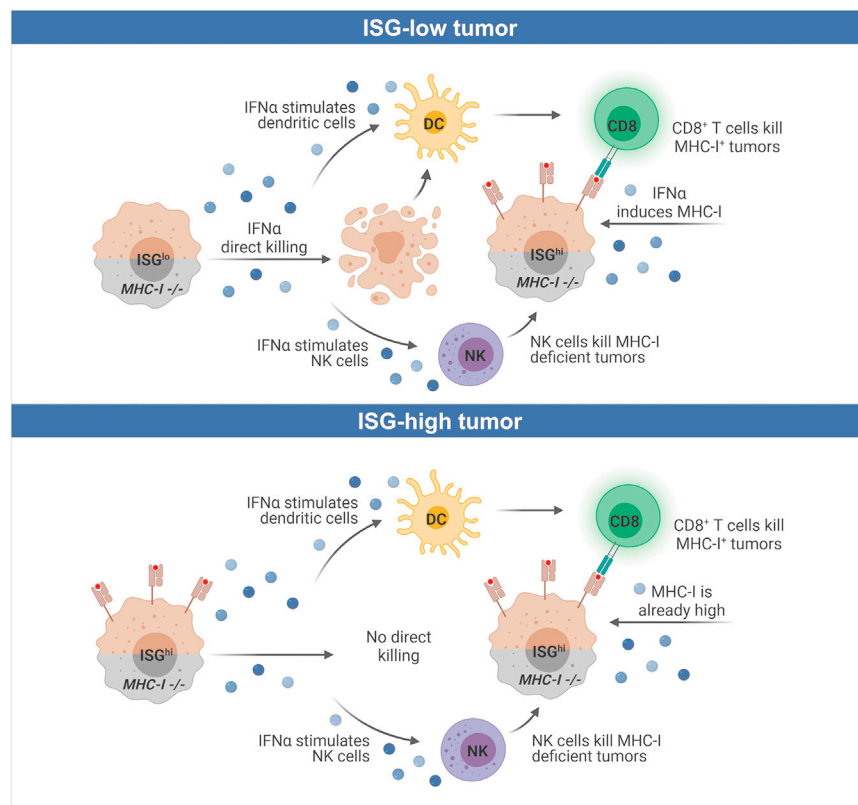
Figure 6. Predicted impact of ISG phenotype on anti-tumor functions of IFNα

(Top) In ISG-low tumors, IFNα directly kills tumor cells, stimulates dendritic cell priming of T cells, increases tumor MHC-I expression, and promotes NK-mediated killing of MHC-I deficient tumors. (Bottom) In ISG-high tumors, direct killing of tumor cells is impaired and there is no IFNα induction of tumor MHC-I expression. The other anti-tumor functions of IFNα are intact. Images were produced using BioRender. DC, dendritic cell; IFN, interferon; ISG-high, high basal expression of interferon-stimulated genes; ISG-low, low basal expression of interferon-stimulated genes; MHC-I, major histocompatibility complex class I.

In this work, we defined a 65-gene IFNα response signature and showed that it segregates IFNα-sensitive and resistant cell lines in an independent dataset composed of cell lines from multiple tumor types, indicating that our findings extend beyond bladder cancer. The presence of type I IFN signatures in tumors is often interpreted to indicate "hot" tumors infiltrated with immune cells;[56,57] however, bioinformatics analysis of primary tumors supports the hypothesis that in a subset of tumors the type I IFN signature could be elevated independently of immune cells. As bulk tissue deconvolution methods are approximate, it is not clear to what extent tumor versus immune cells contribute to whole-tumor type I IFN signatures. Homogeneous sampling methods may not be suitable to determine the presence of ISG-high tumor cells in clinical samples. Single-cell RNA-seq is one method that could potentially be used to determine whether ISG-high tumor cells are present in clinical samples, although a requirement for fresh tissue limits the practicality of this approach. We also identified several individual ISGs as candidate biomarkers that can discriminate bladder cancer cells that are sensitive or resistant to IFNα-induced cytotoxicity and transcriptional response. Future studies employing a targeted approach, such as immunohistochemistry or RNA *in situ* hybridization, to detect expression of individual ISGs in combination with immune-specific markers or histology will be important to determine the clinical relevance of ISG-high tumor cells and the implications for response to type I IFN-based therapies.

inhibitor ligand PD-L1, which inhibits CD8⁺ T cell-mediated killing.[33,34] The gene encoding PD-L1 (*CD274*) was expressed at low levels in both ISG-low and ISG-high cell lines with minimal increases following rhIFNα2b treatment. Thus, while stimulation of the adaptive immune response by type I IFNs is expected to complement immune checkpoint blockade, the outcome of combination therapy may be independent of PD-L1 regulation by type I IFN in tumor cells.

Besides promoting the adaptive anti-tumor immune response, IFNα also increases the anti-tumor activity of NK cells, which preferentially kill cells that lack MHC-I expression ("missing self").[48,49] Indeed, there are several reports describing NK cells as key effectors mediating the anti-tumor effects of type I IFNs,[50–52] although other examples are NK cell-independent.[53,54] As deficiencies in MHC-I genes are common in bladder cancer,[55] NK cells could be a major component of the anti-tumor immune activity of type I IFN-based bladder cancer therapies. NK cell-mediated killing of MHC-I deficient tumor cells is not predicted to be impacted by direct action of type I IFN on tumor cells; however, activation of NK cells by type I IFN in the TME could promote this aspect of anti-tumor immunity (Figure 6). In the context of MHC-I-intact tumor cells, type I IFN could shift the anti-tumor immune response from NK-mediated to T cell-mediated as it increases MHC-I expression in tumor cells. Further work is required to elucidate how type I IFN modulates the TME response to ISG-high versus ISG-low tumors *in vivo*.

MATERIALS AND METHODS
Reagents
Research-grade human serotype 5 adenoviral vectors lacking the E1 and E3 regions were produced by Viraquest Inc. Ad-IFNα2b is a dual expression vector with cytomegalovirus (CMV)-hIFNα2b in the E1 region and RSV-GFP in the E3 region. The Ad-GFP control vector has an empty E1 region and RSV-GFP in the E3 region (Figure 2A). The following other reagents were used in this study: rhIFNα2b (Stem Cell Technologies, 78,077), palbociclib (Cayman, 16,273), rhTRAIL (R&D 375-TL).

Cell lines and cell culture

RT4, UM-UC-4, UM-UC-6, and UM-UC-10 were obtained from EMD. T24, J82, SV-HUC-1, UM-UC-3, SW-780, SCaBER, TCC-SUP, HT-1197, and HT-137 were obtained from ATCC. J82 was cultured in MEM with 10% fetal bovine serum (FBS); T24 and RT4 were cultured in McCoy's 5a with 10% FBS; SV-HUC-1 was cultured in F-12K with 10% FBS; UM-UC-3, UM-UC-4, UM-UC-6, UM-UC-10, TCC-SUP, HT-1376, HT-1197, and SCaBER were cultured in Eagle's minimum essential medium with 10% FBS; and SW-780 was cultured in L-15 with 10% FBS in sealed flasks to prevent air exchange. All cells were maintained in complete growth media at 37°C under 5% CO_2 in a humid environment.

Conditioned media used in cytotoxicity assays was prepared by transducing 3×10^6 SV-HUC-1 cells with Ad-IFNα2b or Ad-GFP at MOI = 100. Transductions were performed in Assay Media (MEM without phenol red, with 2 mM L-glutamine) with 2% FBS in suspension at 37°C for three hours. Media containing virus was removed and cells were plated in T75 flasks with 11 mL Assay Media with 10% FBS and cultured for 72 h. Conditioned media was collected, cell debris was cleared by centrifugation at 1,000 relative centrifugal force (g), then media was sterilized by filtration through a 0.22-μM pore size filter, aliquoted, and stored at −80°C.

Proliferation assays

The Click-iT EdU HCS Assay (Thermo, C10351) was used to measure proliferation. EdU is a nucleoside analog of thymidine and is incorporated into DNA during active DNA synthesis. Cells were seeded at 10,000 cells/well in CellCarrier 96-well plates in 100 μL Assay Media with 10% FBS. The following day, treatments were applied, and cells were incubated for 24 h after which EdU was added to a final concentration of 10 μM followed by incubation for an additional 4 h. Fixation, permeabilization, and DNA staining were performed according to kit instructions. Images were acquired using the ImageXpress Micro Confocal High-Content Imaging System (Molecular Devices) and analyzed using MetaXpress High-Content Image Acquisition and Analysis Software.

Cytotoxicity assays

Cytotoxicity was measured using the CytoToxGlo Assay (Promega, G9291). Cells were seeded at 15,000 cells/well in white wall clear bottom tissue culture (TC-) treated 96 well plates. Virus-treated cells were transduced in Assay Media with 2% FBS immediately after seeding for 3 h at 37°C. Following a 3-h incubation, FBS concentration was adjusted to 10% and cells were incubated for an additional 45 h (48 h total). Other treatments were performed for 48 h in Assay Media containing 10% FBS. Following the 48-h incubation, the CytoToxGlo Assay Reagent was added, and luminescence was measured (LUM signal from dead cells). After the first reading, cells were lysed, and luminescence was measured again (LUM signal from total cells). The fraction of dead cells was determined for each treatment and normalized to the control untreated/mock-infected condition for each cell line.

Cell treatments and RNA preparation

Cells were seeded in six-well TC-treated plates in triplicate. The following day, treatments were applied, and cells were incubated as indicated at 37°C in Assay Media with 10% FBS. Following incubation, media was aspirated fully and 0.6 mL RLT buffer with β-mercaptoethanol (from Qiagen RNeasy Plus kit) was added to wells and plates were frozen at −20°C. Plates were thawed on ice, wells were scraped, and contents transferred to QIAshredder columns. RNA was isolated according to the RNeasy Plus kit instructions (Qiagen). RNA was eluted, quantified, aliquoted for RNA-seq submission and/or qPCR, then frozen at −80°C.

Immunoblots

Cells were seeded in six-well TC-treated plates and grown to 70% to 80% confluence in Assay Media with 10% FBS. Cells were lysed directly in 1X LDS buffer with 5% beta-mercaptoethanol (BME), sonicated, and proceeded to SDS-PAGE. The following primary antibodies were used: glyceraldehyde 3-phosphate dehydrogenase (GAPDH) (Abcam, ab8245), Vimentin (CST, 5741), E-Cadherin (CST, 14,472), PPAR-gamma (CST, 2443), IFNAR1 (Abcam, ab45172), DR4 (CST, 42,533), STAT1 (CST, 14,994), and pTyr701-STAT1 (CST, 9167). Immunoblots were analyzed using the Odyssey LiCor near-infrared imaging system.

Quantitative PCR

One-step RT-qPCR using Taqman Fast Virus 1-Step Master Mix (Thermo, 4,444,434) was performed on the QuantStudio6 instrument in a Duplex reaction with GAPDH using the following Taqman assays: GAPDH, Hs02786624_g1 (Thermo, VIC-MGB_PL), IFI27, Hs01086373_g1 (Thermo, FAM-MGB), STAT1, Hs01013996_m1 (Thermo, FAM-MGB), BST2, Hs00171632_m1 (Thermo, FAM-MGB).

Cell line RNA-seq

The quality of total RNA was evaluated using the Agilent 2100 bioanalyzer (Agilent, Palo Alto, CA) with the RNA 6000 Nano LabChip kit. RNA-seq libraries were prepared with the Illumina TruSeq RNA Library Prep Kit v2 and were sequenced using Illumina NovaSeq to obtain 150-base pair paired-end reads. The sequencing depth for each sample was >20 million reads. The assembly was performed using the nf-core/rnaseq pipeline (1.4.2).[58] Briefly, reads were aligned with Hisat2 (2.1.0) to the human reference build GRCh38 and transcripts were quantified using featureCounts (1.6.4). Feature selection, normalization and differential expression analysis were performed using R(4.0.1)/Bioconductor with the edgeR (3.32.1)[59] and Limma (3.46.0)[60] packages. Prior to differential expression modeling, low expression features were excluded and samples were adjusted by normalization factors, voom-transformed, and further adjusted for correlations between technical replicates using the duplicateCorrelation function in Limma. Genes with BH-adjusted p-value <0.05 and absolute log2 fold-change greater than 1 were taken as significantly differentially expressed. The 65 genes in the bladder cancer cell line rhIFNα2b signature comprise the intersection of the following sets of differentially expressed features: genes upregulated in sensitive

cell lines following treatment with rhIFNα (p.adj <0.05, log2fc > 1) and genes upregulated in untreated ISG-high versus untreated ISG-low cell lines (p.adj <0.05, log2fc > 1). Gene signature scores were computed using singscore (1.10.0).[58] GSEA analysis was performed on the comparison of untreated ISG-high versus ISG-low cell lines sorted and ranked by t-statistic using the Hallmark pathway gene sets from the molecular signatures database (MSigDB v7.4). R visualizations used tidyverse[61] and pheatmap[62] packages.

TCGA analysis

Pre-processed TCGA data were downloaded as batch- and quantile-normalized rsem-fpkm values.[63] IFNα response scores on TCGA primary bladder tumor samples were computed as described above. The score cutoff for ISG-high tumors was derived from the maximum value of the ISG-medium subgroup after using k-means clustering (n = 3) to stratify tumors into ISG-low, ISG-medium, and ISG-high groups. Estimations of tumor purity were obtained from the Genomic Data Commons PanCancerAtlas, which applied the ABSOLUTE method to infer tumor purity from somatic DNA aberrations.[64] Immune and stromal cell infiltration were inferred using the ESTIMATE method.[31] Immune and stromal infiltration scores were each dichotomized into "low" and "high" categories using the mean of each score.

Data and code availability

The RNA-seq data is available at the NCBI Gene Expression Omnibus (GEO): database accession number GSE186611 (https://www.ncbi.nlm.nih.gov/geo/query/acc.cgi?acc=GSE186611). Source code to generate figures is provided at https://github.com/ladyjkalx/IFN-response-manuscript.

AUTHOR CONTRIBUTIONS

J.L.G., R.O., A.K., and S.R.P.M. conceptualized the study. J.L.G. and R.O. developed the methodology. J.L.G., A.L.K., and C.M. validated the study. J.L.G., R.O., A.L.K., and C.M. completed the formal analysis. J.L.G., R.O., A.L.K., C.M., and R.B.Z. performed the investigation. R.O. performed the data curation. J.L.G. and R.O. wrote the original draft. J.L.G., R.O., A.K., S.R.P.M., B.C.F., J.S.J., A.L.K., and C.M. reviewed and edited the manuscript. J.L.G., R.O., A.L.K., and C.M. visualized the study. J.L.G., S.R.P.M., B.C.F., and A.K. supervised the study. J.L.G. and A.K. performed project administration.

DECLARATION OF INTERESTS

All authors are current or former employees of Ferring Pharmaceuticals.

REFERENCES

1. Babjuk, M., Burger, M., Comperat, E.M., Gontero, P., Mostafid, A.H., Palou, J., van Rhijn, B.W.G., Roupret, M., Shariat, S.F., Sylvester, R., et al. (2019). European association of urology guidelines on non-muscle-invasive bladder cancer (TaT1 and carcinoma in situ) - 2019 update. Eur. Urol. 76, 639–657. https://doi.org/10.1016/j.eururo.2019.08.016.

2. Sylvester, R.J., Brausi, M.A., Kirkels, W.J., Hoeltl, W., Calais Da Silva, F., Powell, P.H., Prescott, S., Kirkali, Z., van de Beek, C., Gorlia, T., et al. (2010). Long-term efficacy results of EORTC genito-urinary group randomized phase 3 study 30911 comparing intravesical instillations of epirubicin, bacillus Calmette-Guérin, and bacillus Calmette-Guérin plus isoniazid in patients with intermediate- and high-risk stage Ta T1 urothelial carcinoma of the bladder. Eur. Urol. 57, 766–773. https://doi.org/10.1016/j.eururo.2009.12.024.

3. Iqbal Ahmed, C.M., Johnson, D.E., Demers, G.W., Engler, H., Howe, J.A., Wills, K.N., Wen, S.F., Shinoda, J., Beltran, J., Nodelman, M., et al. (2001). Interferon alpha2b gene delivery using adenoviral vector causes inhibition of tumor growth in xenograft models from a variety of cancers. Cancer Gene Ther. 8, 788–795. https://doi.org/10.1038/sj.cgt.7700364.

4. Connor, R.J., Anderson, J.M., Machemer, T., Maneval, D.C., and Engler, H. (2005). Sustained intravesical interferon protein exposure is achieved using an adenoviral-mediated gene delivery system: a study in rats evaluating dosing regimens. Urology 66, 224–229. https://doi.org/10.1016/j.urology.2005.02.015.

5. Boorjian, S.A., Alemozaffar, M., Konety, B.R., Shore, N.D., Gomella, L.G., Kamat, A.M., Bivalacqua, T.J., Montgomery, J.S., Lerner, S.P., Busby, J.E., et al. (2021). Intravesical nadofaragene firadenovec gene therapy for BCG-unresponsive non-muscle-invasive bladder cancer: a single-arm, open-label, repeat-dose clinical trial. Lancet Oncol. 22, 107–117. https://doi.org/10.1016/S1470-2045(20)30540-4.

6. Shore, N.D., Boorjian, S.A., Canter, D.J., Ogan, K., Karsh, L.I., Downs, T.M., Gomella, L.G., Kamat, A.M., Lotan, Y., Svatek, R.S., et al. (2017). Intravesical rAd-IFNalpha/syn3 for patients with high-grade, Bacillus calmette-guerin-refractory or relapsed non-muscle-invasive bladder cancer: a phase II randomized study. J. Clin. Oncol. 35, 3410–3416. https://doi.org/10.1200/JCO.2017.72.3064.

7. Borden, E.C. (2019). Interferons alpha and beta in cancer: therapeutic opportunities from new insights. Nat. Rev. Drug Discov. 18, 219–234. https://doi.org/10.1038/s41573-018-0011-2.

8. Parker, B.S., Rautela, J., and Hertzog, P.J. (2016). Antitumour actions of interferons: implications for cancer therapy. Nat. Rev. Cancer 16, 131–144. https://doi.org/10.1038/nrc.2016.14.

9. Medrano, R.F.V., Hunger, A., Mendonca, S.A., Barbuto, J.A.M., and Strauss, B.E. (2017). Immunomodulatory and antitumor effects of type I interferons and their application in cancer therapy. Oncotarget 8, 71249–71284. https://doi.org/10.18632/oncotarget.19531.

10. Blank, C., Brown, I., Peterson, A.C., Spiotto, M., Iwai, Y., Honjo, T., and Gajewski, T.F. (2004). PD-L1/B7H-1 inhibits the effector phase of tumor rejection by T cell receptor (TCR) transgenic CD8+ T cells. Cancer Res. 64, 1140–1145. https://doi.org/10.1158/0008-5472.can-03-3259.

11. Uzhachenko, R.V., and Shanker, A. (2019). CD8(+) T Lymphocyte and NK cell network: circuitry in the cytotoxic domain of immunity. Front Immunol. 10, 1906. https://doi.org/10.3389/fimmu.2019.01906.

12. Papageorgiou, A., Lashinger, L., Millikan, R., Grossman, H.B., Benedict, W., Dinney, C.P.N., and McConkey, D.J. (2004). Role of tumor necrosis factor-related apoptosis-inducing ligand in interferon-induced apoptosis in human bladder cancer cells. Cancer Res. 64, 8973–8979. https://doi.org/10.1158/0008-5472.Can-04-1909.

13. Grups, J.W., and Frohmuller, H.G. (1988). Antiproliferative effects of interferons against human bladder carcinoma cell lines in vitro. Urol. Int. 43, 265–268. https://doi.org/10.1159/000281351.

14. Hubbell, H.R., Liu, R.S., and Maxwell, B.L. (1984). Independent sensitivity of human tumor cell lines to interferon and double-stranded RNA. Cancer Res. 44, 3252–3257.

15. Benedict, W.F., Tao, Z., Kim, C.S., Zhang, X., Zhou, J.H., Adam, L., McConkey, D.J., Papageorgiou, A., Munsell, M., Philopena, J., et al. (2004). Intravesical Ad-IFNalpha causes marked regression of human bladder cancer growing orthotopically in nude mice and overcomes resistance to IFN-alpha protein. Mol. Ther. 10, 525–532. https://doi.org/10.1016/j.ymthe.2004.05.027.

16. Zhang, X., Dong, L., Chapman, E., and Benedict, W.F. (2008). Conditioned medium from Ad-IFN-alpha-infected bladder cancer and normal urothelial cells is cytotoxic to cancer cells but not normal cells: further evidence for a strong bystander effect. Cancer Gene Ther. *15*, 817–822. https://doi.org/10.1038/cgt.2008.53.

17. Zhang, X., Yang, Z., Dong, L., Papageorgiou, A., McConkey, D.J., and Benedict, W.F. (2007). Adenoviral-mediated interferon alpha overcomes resistance to the interferon protein in various cancer types and has marked bystander effects. Cancer Gene Ther. *14*, 241–250. https://doi.org/10.1038/sj.cgt.7701011.

18. Rigby, C.C.; Franks, L.M (1970). A human tissue culture cell line from a transitional cell tumour of the urinary bladder: growth, chromosome pattern and ultrastructure. Br. J. Cancer *24*, 746–754.

19. Grossman, H.B.; Wedemeyer, G., Ren, L., Wilson, G.N., and Cox, B (1986). Improved growth of human urothelial carcinoma cell cultures. J Urol *136*, 953–959. https://doi.org/10.1016/s0022-5347(17)45139-1.

20. Kyriazis, A.A.; Kyriazis, A.P., Sternberg, C.N., Sloane, N.H., and Loveless, J.D (1986). Morphological, biological, biochemical, and karyotypic characteristics of human pancreatic ductal adenocarcinoma Capan-2 in tissue culture and the nude mouse. Cancer Res *46*, 5810–5815.

21. Sabichi, A.; Keyhani, A., Tanaka, N., Delacerda, J., Lee, I.L., Zou, C., Zhou, J.H., Benedict, W.F., and Grossman, H.B (2006). Characterization of a panel of cell lines derived from urothelial neoplasms: genetic alterations, growth in vivo and the relationship of adenoviral mediated gene transfer to coxsackie adenovirus receptor expression. J Urol *175*, 1133–1137.

22. Nayak, S.K.; O'Toole, C., and Price, Z.H (1977). A cell line from an anaplastic transitional cell carcinoma of human urinary bladder. Br J Cancer, 142–151.

23. Bubenik, J.; Baresova, M., Viklicky, V., Jakoubkova, J., Sainerova, H., and Donner, J (1973). Established cell line of urinary bladder carcinoma (T24) containing tumour-specific antigen. Int J Cancer *11*, 765–773.

24. O'Toole, C.; Nayak, S., Price, Z., Gilbert, W.H., and Waisman, J (1976). A cell line (SCABER) derived from squamous cell carcinoma of the human urinary bladder. Int J Cancer *17*, 707–714.

25. Rasheed, S.; Gardner, M.B., Rongey, R.W., Nelson-Rees, W.A., and Arnstein, P (1977). Human bladder carcinoma: characterization of two new tumor cell lines and search for tumor viruses. J Natl Cancer Inst *58*, 881–890.

26. O'Toole, C.; Price, Z.H., Ohnuki, Y., and Unsgaard, B (1978). Ultrastructure, karyology and immunology of a cell line originated from a human transitional-cell carcinoma. Br J Cancer *38*, 64–76.

27. Kamoun, A., de Reynies, A., Allory, Y., Sjodahl, G., Robertson, A.G., Seiler, R., Hoadley, K.A., Groeneveld, C.S., Al-Ahmadie, H., Choi, W., et al. (2020). A consensus molecular classification of muscle-invasive bladder cancer. Eur. Urol. *77*, 420–433. https://doi.org/10.1016/j.eururo.2019.09.006.

28. Long, Q., Ma, A.H., Zhang, H., Cao, Z., Xia, R., Lin, T.Y., Sonpavde, G.P., de Vere White, R., Guo, J., and Pan, C.X. (2020). Combination of cyclin-dependent kinase and immune checkpoint inhibitors for the treatment of bladder cancer. Cancer Immunol. Immunother. *69*, 2305–2317. https://doi.org/10.1007/s00262-020-02609-5.

29. Siegrist, F., Ebeling, M., and Certa, U. (2011). The small interferon-induced transmembrane genes and proteins. J. Interferon Cytokine Res. *31*, 183–197. https://doi.org/10.1089/jir.2010.0112.

30. Aran, D., Sirota, M., and Butte, A.J. (2015). Systematic pan-cancer analysis of tumour purity. Nat. Commun. *6*, 8971. https://doi.org/10.1038/ncomms9971.

31. Yoshihara, K., Shahmoradgoli, M., Martinez, E., Vegesna, R., Kim, H., Torres-Garcia, W., Trevino, V., Shen, H., Laird, P.W., Levine, D.A., et al. (2013). Inferring tumour purity and stromal and immune cell admixture from expression data. Nat. Commun. *4*, 2612. https://doi.org/10.1038/ncomms3612.

32. Liu, H., Golji, J., Brodeur, L.K., Chung, F.S., Chen, J.T., deBeaumont, R.S., Bullock, C.P., Jones, M.D., Kerr, G., Li, L., et al. (2019). Tumor-derived IFN triggers chronic pathway agonism and sensitivity to ADAR loss. Nat. Med. *25*, 95–102. https://doi.org/10.1038/s41591-018-0302-5.

33. Terawaki, S., Chikuma, S., Shibayama, S., Hayashi, T., Yoshida, T., Okazaki, T., and Honjo, T. (2011). IFN-alpha directly promotes programmed cell death-1 transcription and limits the duration of T cell-mediated immunity. J. Immunol. *186*, 2772–2779. https://doi.org/10.4049/jimmunol.1003208.

34. Plote, D., Choi, W., Mokkapati, S., Sundi, D., Ferguson, J.E., Duplisea, J., Parker, N.R., Yla-Herttuala, S., Committee, S.C.B., McConkey, D., et al. (2019). Inhibition of urothelial carcinoma through targeted type I interferon-mediated immune activation. Oncoimmunology *8*, e1577125.

35. Lu, C., Guan, J., Lu, S., Jin, Q., Rousseau, B., Lu, T., Stephens, D., Zhang, H., Zhu, J., Yang, M., et al. (2021). DNA sensing in mismatch repair-deficient tumor cells is essential for anti-tumor immunity. Cancer Cell *39*, 96–108.e106. https://doi.org/10.1016/j.ccell.2020.11.006.

36. Grups, J.W., and Bange, F.C. (1990). Interferon receptors on the surface of interferon-sensitive and interferon-resistant urothelial carcinomas. Urol. Res. *18*, 119–122. https://doi.org/10.1007/BF00302471.

37. Arimoto, K.I., Miyauchi, S., Stoner, S.A., Fan, J.B., and Zhang, D.E. (2018). Negative regulation of type I IFN signaling. J. Leukoc. Biol. https://doi.org/10.1002/JLB.2MIR0817–342R.

38. McConkey, D.J., Choi, W., Marquis, L., Martin, F., Williams, M.B., Shah, J., Svatek, R., Das, A., Adam, L., Kamat, A., et al. (2009). Role of epithelial-to-mesenchymal transition (EMT) in drug sensitivity and metastasis in bladder cancer. Cancer Metastasis Rev. *28*, 335–344. https://doi.org/10.1007/s10555-009-9194-7.

39. Choi, W., Porten, S., Kim, S., Willis, D., Plimack, E.R., Hoffman-Censits, J., Roth, B., Cheng, T., Tran, M., Lee, I.L., et al. (2014). Identification of distinct basal and luminal subtypes of muscle-invasive bladder cancer with different sensitivities to frontline chemotherapy. Cancer Cell *25*, 152–165. https://doi.org/10.1016/j.ccr.2014.01.009.

40. Warrick, J.I., Walter, V., Yamashita, H., Chung, E., Shuman, L., Amponsa, V.O., Zheng, Z., Chan, W., Whitcomb, T.L., Yue, F., et al. (2016). FOXA1, GATA3 and PPAR cooperate to drive luminal subtype in bladder cancer: a molecular analysis of established human cell lines. Sci. Rep. *6*, 38531. https://doi.org/10.1038/srep38531.

41. Michalska, A., Blaszczyk, K., Wesoly, J., and Bluyssen, H.A.R. (2018). A positive feedback amplifier circuit that regulates interferon (IFN)-Stimulated gene expression and controls type I and type II IFN responses. Front Immunol. *9*, 1135. https://doi.org/10.3389/fimmu.2018.01135.

42. Stark, G.R., Kerr, I.M., Williams, B.R., Silverman, R.H., and Schreiber, R.D. (1998). How cells respond to interferons. Annu. Rev. Biochem. *67*, 227–264. https://doi.org/10.1146/annurev.biochem.67.1.227.

43. Wang, W., Yin, Y., Xu, L., Su, J., Huang, F., Wang, Y., Boor, P.P.C., Chen, K., Wang, W., Cao, W., et al. (2017). Unphosphorylated ISGF3 drives constitutive expression of interferon-stimulated genes to protect against viral infections. Sci. Signal *10*, eaah4248. https://doi.org/10.1126/scisignal.aah4248.

44. Munafo, A., Trinchard-Lugan, I.I., Nguyen, T.X., and Buraglio, M. (1998). Comparative pharmacokinetics and pharmacodynamics of recombinant human interferon beta-1a after intramuscular and subcutaneous administration. Eur. J. Neurol. *5*, 187–193. https://doi.org/10.1046/j.1468-1331.1998.520187.x.

45. Buchwalder, P.A., Buclin, T., Trinchard, I., Munafo, A., and Biollaz, J. (2000). Pharmacokinetics and pharmacodynamics of IFN-beta 1a in healthy volunteers. J. Interferon Cytokine Res. *20*, 857–866. https://doi.org/10.1089/10799900050163226.

46. Garcia-Garcia, I., Gonzalez-Delgado, C.A., Valenzuela-Silva, C.M., Diaz-Machado, A., Cruz-Diaz, M., Nodarse-Cuni, H., Perez-Perez, O., Bermudez-Badell, C.H., Ferrero-Bibilonia, J., Paez-Meireles, R., et al. (2010). Pharmacokinetic and pharmacodynamic comparison of two "pegylated" interferon alpha-2 formulations in healthy male volunteers: a randomized, crossover, double-blind study. BMC Pharmacol. *10*, 15. https://doi.org/10.1186/1471-2210-10-15.

47. Bruno, R., Sacchi, P., Scagnolari, C., Torriani, F., Maiocchi, L., Patruno, S., Bellomi, F., Filice, G., and Antonelli, G. (2007). Pharmacodynamics of peginterferon alpha-2a and peginterferon alpha-2b in interferon-naive patients with chronic hepatitis C: a randomized, controlled study. Aliment. Pharmacol. Ther. *26*, 369–376. https://doi.org/10.1111/j.1365-2036.2007.03392.x.

48. Marcus, A., Gowen, B.G., Thompson, T.W., Iannello, A., Ardolino, M., Deng, W., Wang, L., Shifrin, N., and Raulet, D.H. (2014). Recognition of tumors by the innate immune system and natural killer cells. Adv. Immunol. *122*, 91–128. https://doi.org/10.1016/B978-0-12-800267-4.00003-1.

49. Ljunggren, H.G., and Karre, K. (1990). In search of the 'missing self': MHC molecules and NK cell recognition. Immunol. Today *11*, 237–244. https://doi.org/10.1016/0167-5699(90)90097-s.

50. Qin, X.Q., Beckham, C., Brown, J.L., Lukashev, M., and Barsoum, J. (2001). Human and mouse IFN-beta gene therapy exhibits different anti-tumor mechanisms in mouse models. Mol. Ther. *4*, 356–364. https://doi.org/10.1006/mthe.2001.0464.

51. Narumi, K., Kondoh, A., Udagawa, T., Hara, H., Goto, N., Ikarashi, Y., Ohnami, S., Okada, T., Yamagishi, M., Yoshida, T., and Aoki, K. (2010). Administration route-dependent induction of antitumor immunity by interferon-alpha gene transfer. Cancer Sci. *101*, 1686–1694. https://doi.org/10.1111/j.1349-7006.2010.01578.x.

52. Tada, H., Maron, D.J., Choi, E.A., Barsoum, J., Lei, H., Xie, Q., Liu, W., Ellis, L., Moscioni, A.D., Tazelaar, J., et al. (2001). Systemic IFN-beta gene therapy results in long-term survival in mice with established colorectal liver metastases. J. Clin. Invest. *108*, 83–95. https://doi.org/10.1172/JCI9841.

53. Odaka, M., Sterman, D.H., Wiewrodt, R., Zhang, Y., Kiefer, M., Amin, K.M., Gao, G.P., Wilson, J.M., Barsoum, J., Kaiser, L.R., and Albelda, S.M. (2001). Eradication of intraperitoneal and distant tumor by adenovirus-mediated interferon-beta gene therapy is attributable to induction of systemic immunity. Cancer Res. *61*, 6201–6212.

54. Odaka, M., Wiewrodt, R., DeLong, P.A., Tanaka, T., Zhang, Y., Kaiser, L.R., and Albelda, S.M. (2002). Analysis of the immunologic response generated by Ad.IFN-β during successful intraperitoneal tumor gene therapy. Mol. Ther. *6*, 210–218. https://doi.org/10.1006/mthe.2002.0656.

55. Maleno, I., Aptsiauri, N., Cabrera, T., Gallego, A., Paschen, A., Lopez-Nevot, M.A., and Garrido, F. (2011). Frequent loss of heterozygosity in the beta2-microglobulin region of chromosome 15 in primary human tumors. Immunogenetics *63*, 65–71. https://doi.org/10.1007/s00251-010-0494-4.

56. Woo, S.R., Corrales, L., and Gajewski, T.F. (2015). The STING pathway and the T cell-inflamed tumor microenvironment. Trends Immunol. *36*, 250–256. https://doi.org/10.1016/j.it.2015.02.003.

57. Gajewski, T.F., Schreiber, H., and Fu, Y.X. (2013). Innate and adaptive immune cells in the tumor microenvironment. Nat. Immunol. *14*, 1014–1022. https://doi.org/10.1038/ni.2703.

58. Ewels, P.A., Peltzer, A., Fillinger, S., Patel, H., Alneberg, J., Wilm, A., Garcia, M.U., Di Tommaso, P., and Nahnsen, S. (2020). The nf-core framework for community-curated bioinformatics pipelines. Nat. Biotechnol. *38*, 276–278. https://doi.org/10.1038/s41587-020-0439-x.

59. McCarthy, D.J., Chen, Y., and Smyth, G.K. (2012). Differential expression analysis of multifactor RNA-Seq experiments with respect to biological variation. Nucleic Acids Res. *40*, 4288–4297. https://doi.org/10.1093/nar/gks042.

60. Ritchie, M.E., Phipson, B., Wu, D., Hu, Y., Law, C.W., Shi, W., and Smyth, G.K. (2015). Limma powers differential expression analyses for RNA-sequencing and microarray studies. Nucleic Acids Res. *43*, e47. https://doi.org/10.1093/nar/gkv007.

61. Wickham, H., Averick, M., Bryan, J., Chang, W., McGowan, L.D.A., François, R., et al. (2019). Welcome to the tidyverse. J. Open Source Softw. *4*, 1686. https://doi.org/10.21105/joss.01686.

62. Kolde, R. (2019). Package 'pheatmap'. Available at: https://cran.r-project.org/web/packages/pheatmap/index.html. Accessed September 15, 2021 (Pheatmap).

63. Wang, Q., Armenia, J., Zhang, C., Penson, A.V., Reznik, E., Zhang, L., Minet, T., Ochoa, A., Gross, B.E., Iacobuzio-Donahue, C.A., et al. (2018). Unifying cancer and normal RNA sequencing data from different sources. Sci. Data *5*, 180061. https://doi.org/10.1038/sdata.2018.61.

64. Carter, S.L., Cibulskis, K., Helman, E., McKenna, A., Shen, H., Zack, T., Laird, P.W., Onofrio, R.C., Winckler, W., Weir, B.A., et al. (2012). Absolute quantification of somatic DNA alterations in human cancer. Nat. Biotechnol. *30*, 413–421. https://doi.org/10.1038/nbt.2203.